



Personalized circulating tumor DNA analysis as a predictive biomarker in solid tumor patients treated with pembrolizumab

Scott V. Bratman^{1,2,3,9}, S. Y. Cindy Yang^{1,3,9}, Marco A. J. Lafolla^{3,4}, Zhihui Liu^{3,5}, Aaron R. Hansen^{3,4}, Philippe L. Bedard^{3,4}, Stephanie Lheureux^{3,4}, Anna Spreafico^{3,4}, Albiruni Abdul Razak^{3,4}, Svetlana Shchegrova⁶, Maggie Louie⁶, Paul Billings⁶, Bernhard Zimmermann⁶, Himanshu Sethi⁶, Alexey Aleshin⁶, Dax Torti⁷, Kayla Marsh⁷, Jenna Eagles⁷, Iulia Cirlan³, Youstina Hanna³, Derek L. Clouthier³, Scott C. Lien^{3,8}, Pamela S. Ohashi^{3,8}, Wei Xu^{3,5}, Lillian L. Siu^{3,4}✉ and Trevor J. Pugh^{1,3,7}✉

Immune checkpoint blockade (ICB) provides clinical benefit to a subset of patients with cancer. However, existing biomarkers do not reliably predict treatment response across diverse cancer types. Limited data exist to show how serial circulating tumor DNA (ctDNA) testing may perform as a predictive biomarker in patients receiving ICB. We conducted a prospective phase II clinical trial to assess ctDNA in five distinct cohorts of patients with advanced solid tumors treated with pembrolizumab (NCT02644369). We applied bespoke ctDNA assays to 316 serial plasma samples obtained at baseline and every three cycles from 94 patients. Baseline ctDNA concentration correlated with progression-free survival, overall survival, clinical response and clinical benefit. This association became stronger when considering ctDNA kinetics during treatment. All 12 patients with ctDNA clearance during treatment were alive with median 25 months follow up. This study demonstrates the potential for broad clinical utility of ctDNA-based surveillance in patients treated with ICB.

ICB using inhibitors of programmed death-1 or its ligand (anti-PD-1/PD-L1) has emerged as an effective therapy for many cancer types. However, a minority of patients (<20%) respond to treatment or have durable clinical benefit. Numerous classes of biomarkers have been proposed¹⁻⁷, but there is no robust predictive marker of treatment response. Early determination of response to ICB could enable patients who are deriving clinical benefit to continue therapy while sparing others from unnecessary toxicities and cost. Standard radiologic criteria for response to these agents do not consistently capture the dynamics of clinical benefit over time⁸⁻¹⁰. Moreover, repeated tumor biopsies are usually not feasible, may be difficult to time appropriately, and may not add meaningful predictive information early in the treatment course. This forms a strong rationale to pursue new noninvasive biomarkers of ICB response that can provide predictive value and/or early determination of clinical benefit.

ctDNA within peripheral blood plasma provides noninvasive access to cancer-specific somatic mutations¹¹. This class of biomarkers is poised to revolutionize the management of patients with advanced cancer by replacing tissue biopsy for noninvasive genotyping of specific mutations that are linked with therapeutic response. Despite its potential, ctDNA has not yet been clinically implemented for patients treated with ICB¹². Proof-of-principle studies suggest that ctDNA quantification and on-treatment changes could

assist in prognostication and response monitoring¹³⁻²¹, but the robustness of these findings have been limited by small cohort sizes, heterogeneous treatment regimens and variable ctDNA detection methodologies.

Here, we present the results of a prospective clinical trial of ICB in distinct cohorts of advanced solid tumors. We evaluated the performance of an amplicon-based bespoke ctDNA detection platform for prognostication and response monitoring in patients treated with the anti-PD-1 monoclonal antibody, pembrolizumab. We hypothesized that (1) baseline ctDNA levels would be prognostic and (2) early changes in ctDNA levels would precede radiographic response. Our findings could help advance the implementation of ctDNA-based testing in the context of ICB treatment across cancer types.

Results

A multi-cohort clinical trial of ICB in advanced solid tumors.

We conducted a single-institution phase II study of pembrolizumab in patients with advanced solid tumors (investigator-initiated phase II study of pembrolizumab immunological response evaluation (INSPIRE), NCT02644369)²². Five parallel cohorts were included: squamous cell cancer of head and neck (SCCHN), triple negative breast cancer (TNBC), high-grade serous ovarian cancer (HGSOC), malignant melanoma and mixed solid tumors (MST)

¹Department of Medical Biophysics, University of Toronto, Toronto, Ontario, Canada. ²Department of Radiation Oncology, University of Toronto, Toronto, Ontario, Canada. ³Princess Margaret Cancer Centre, University Health Network, Toronto, Ontario, Canada. ⁴Division of Medical Oncology, Department of Medicine, University of Toronto, Toronto, Ontario, Canada. ⁵Dalla Lana School of Public Health, University of Toronto, Toronto, Ontario, Canada. ⁶Natera, Inc., San Carlos, CA, USA. ⁷Ontario Institute of Cancer Research, Toronto, Ontario, Canada. ⁸Department of Immunology, University of Toronto, Toronto, Ontario, Canada. ⁹These authors contributed equally: Scott V. Bratman, S. Y. Cindy Yang. ✉e-mail: lillian.siu@uhn.ca; trevor.pugh@utoronto.ca

(Supplementary Table 1). In designing this study, a prespecified objective was to assess the feasibility of using ctDNA as an indicator of tumor burden in patients with advanced solid tumors being treated with pembrolizumab. Biospecimens were prospectively collected using optimized protocols to ensure high quality for ctDNA analysis (Methods).

A total of 106 patients were enrolled, with 94 (89%) patients having sufficient tumor tissue for the exome sequence analysis that was necessary to design bespoke ctDNA assays (Extended Data Fig. 1). Patients had a median age of 59 years and most were female (62%) and Caucasian (83%) (Supplementary Tables 2 and 3). Before pembrolizumab treatment, patients received a median of two lines of cancer treatment (range 0–6). The median number of pembrolizumab treatment cycles was three (range 1–35), and median follow up was 13.8 months (range 0.6–35.4). Median overall survival (OS) and progression-free survival (PFS) were 14.0 and 1.9 months, respectively. Sixteen (17%) patients experienced complete response ($N=3$) or partial response ($N=13$) (objective response rate (ORR): complete or partial response) and 24 (26%) derived clinical benefit (clinical benefit rate (CBR): complete response, partial response or stable disease for ≥ 6 cycles).

Bespoke ctDNA assays performed at baseline are sensitive and prognostic. Whole-exome sequencing (WES) was performed on protocol-mandated fresh-frozen tumor biopsy tissue obtained within 4 weeks of treatment initiation ($n=71$ patients) or, if insufficient material was available from the protocol-mandated biopsy, on archival tumor tissue obtained 1–83 months before treatment initiation ($n=23$ patients). In each case, matched germline WES was performed to identify tumor-specific somatic mutations (median 2.0 nonsynonymous somatic mutations per megabase pair, range 0.47–187.02). The mutation burden varied within individual cohorts with malignant melanoma displaying the highest rate (Extended Data Fig. 2a).

For each patient, we selected up to 16 clonal somatic mutations for personalized ctDNA assay design²³. Baseline ctDNA (ctDNA_B) was detected in 92 of 94 (98%) samples (Supplementary Table 3); of note, random selection of one of the 16 mutations would have resulted in detection of ctDNA_B in only 84% of cases (Extended Data Fig. 2b,c). Among positive ctDNA_B samples, the median number of detectable mutations was 16 (range 2–16), and 86% had ≥ 10 detectable mutations. The number of detectable mutations at baseline was not significantly different between patients with available fresh-frozen tumor biopsy tissue and patients with archival tumor tissue ($P=0.94$; Extended Data Fig. 2d).

The variant allele frequencies of individual detected mutations ranged from 0.034 to 76.0% (median 5.09%). To more accurately quantify low levels of ctDNA, we calculated mean variant allele frequencies from all tested variants ($N=16$), including the undetected targets (Extended Data Fig. 3). This approach revealed ctDNA_B levels down to 0.004% and 0.07 mean tumor molecules (MTM) per ml of plasma (Extended Data Fig. 4 and Supplementary Table 4); a dynamic range of approximately five orders of magnitude was observed among ctDNA_B levels.

ctDNA_B levels varied among the five cohorts, with highest levels observed in patients with TNBC and MST and lowest levels in patients with malignant melanoma (Extended Data Fig. 4). Although there was considerable variability within each cohort (at least three orders of magnitude), TNBC was the only cohort in which all patients had ctDNA_B > 1 MTM per ml. There was no statistically significant correlation ($P=0.06$) between ctDNA_B levels and the baseline response evaluation criteria in solid tumors (RECIST) target lesion measurements (Extended Data Fig. 4d).

Lower-than-median ctDNA_B levels were associated with superior OS (hazard ratio adjusted for cohort (aHR) 0.49, 95% confidence interval (CI) 0.29–0.83) and PFS (aHR 0.54, 95% CI

0.34–0.85) (Fig. 1a,b and Supplementary Table 5). CBR was significantly higher among patients with ctDNA_B levels below the median for the cohort (OR=3.24, 95% CI 1.19–8.8) and ORR displayed a similar, albeit nonsignificant, trend (OR=2.57, 95% CI 0.82–8.08) (Supplementary Table 5). Subset analysis according to cohort was limited by small sample size (Fig. 1c,d).

Change in ctDNA levels from baseline are predictive of benefit to ICB across cancer types. We next asked whether early, dynamic changes in ctDNA levels were predictive of benefit to ICB. We analyzed ctDNA levels at beginning of cycle 3 (ctDNA_{C3}) of pembrolizumab treatment (week 6–7 for most patients, Fig. 2) in 74 patients with available plasma (Extended Data Fig. 1). Thirty-three patients (45%) had a decrease in ctDNA levels from baseline (Fig. 2). In comparison to absolute ctDNA_B and ctDNA_{C3} values, the relative change in ctDNA levels from baseline to C3 (Δ ctDNA_{C3}) displayed less variability across cancer types (Extended Data Fig. 4a–c).

We analyzed the correlation of early ctDNA kinetics with patient outcomes during ICB treatment. One patient was excluded from this analysis due to lack of detectable ctDNA at both baseline and C3 (Extended Data Fig. 1). Among the remaining 73 patients, Δ ctDNA_{C3} was predictive of ICB benefit across the cohorts. Fourteen (42%) of the 33 patients with negative Δ ctDNA_{C3} (that is, a lower ctDNA level at C3 versus baseline) achieved an objective response, whereas only one (2%) of the 40 patients with positive Δ ctDNA_{C3} had an objective response (odds ratio (OR) 28.74, 95% CI 3.51–253.04). The Δ ctDNA_{C3} was also associated with higher CBR (Supplementary Table 6 and Extended Data Fig. 5) and favorable OS (aHR 0.36, 95% CI 0.18–0.71) and PFS (aHR 0.33, 95% CI 0.19–0.58) (Fig. 3a,b). For both OS and PFS, similar associations with Δ ctDNA_{C3} were observed in each cohort (Fig. 3c,d).

Association of Δ ctDNA_{C3} with clinical outcomes is independent of other putative ICB biomarkers. To evaluate whether the value of ctDNA as a therapeutic biomarker was independent of other putative biomarkers, we compared ctDNA_B and Δ ctDNA_{C3} with tumor mutational burden (TMB) and PD-L1 staining by immunohistochemistry. Both ctDNA metrics displayed weak but statistically significant negative correlations with PD-L1 staining, whereas no significant correlations were observed with TMB (Extended Data Fig. 6a). The strong associations between Δ ctDNA_{C3} and OS, PFS, ORR and CBR were maintained in multivariable models incorporating TMB and/or PD-L1 (Supplementary Table 7). Inclusion of Δ ctDNA_{C3} also improved the accuracy of multivariable models containing TMB, PD-L1 and ctDNA_B (Extended Data Fig. 6b). Only two of 94 patients had microsatellite instability high (MSI-H) tumors (confirmed by clinical immunohistochemistry and tumor WES data), suggesting that the prognostic/predictive value of ctDNA quantification would be applicable to microsatellite stable patients. Taken together, compared with static biomarkers assessed at baseline, an early on-treatment change in ctDNA level is a more informative and generalizable therapeutic biomarker for patients with a variety of solid tumor types treated with ICB.

Combination of cycle 3 RECIST and Δ ctDNA_{C3} refines risk groupings. Patients who progress very early in the course of ICB treatment represent a challenging clinical scenario as it can be difficult to ascertain whether continued treatment may eventually be effective and extend survival. We therefore examined the group of INSPIRE patients with serial ctDNA values and asked whether early ctDNA kinetics could provide added clinical utility beyond early clinical response assessment. Thirty-seven (51%) patients experienced early RECIST progressive disease (PD) by C3 (Fig. 4). Of these, the 30 patients with an increase in ctDNA at C3 (that is, positive Δ ctDNA_{C3}) displayed the shortest survival times despite 11 out of 30 (37%) being treated beyond C3 (median (range) additional

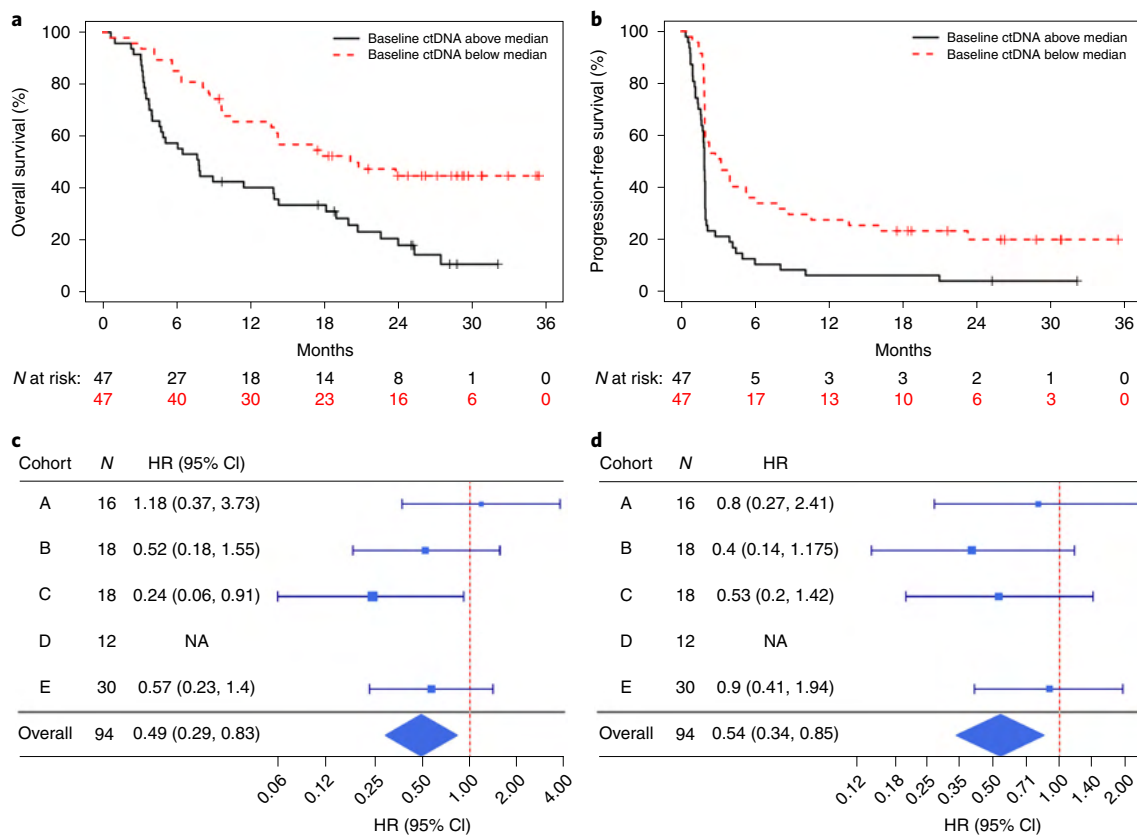


Fig. 1 | Baseline ctDNA level is correlated with OS and PFS. a,b, Kaplan–Meier curves of OS (**a**) or PFS (**b**) in the entire cohort ($N=94$ patients) stratified at the median ctDNA_B value. **c,d**, Forest plots depict the prognostic association of ctDNA_B with OS (**c**) or PFS (**d**) in the five subcohorts. The unadjusted hazard ratios (HR) (squares) and 95% CIs (horizontal lines) are shown for each subcohort. NA, hazard ratio is undefined for cohort D because all events were in the ctDNA_B-above-median group. The overall adjusted hazard ratios with 95% confidence intervals for ctDNA_B after accounting for the cohorts are shown (diamonds). Vertical dotted line indicates the null hypothesis.

pembrolizumab cycles, 2 (1–3)). In retrospect, such continued ICB treatment may have been unnecessary in this poor prognosis subset (early PD, positive Δ ctDNA_{C3}). Furthermore, in this cohort, none of the patients with an increase in both ctDNA and tumor imaging achieved objective response either at first radiological assessment or any time thereafter. In contrast, the seven patients with early RECIST PD with a negative Δ ctDNA_{C3} displayed numerically longer survival times despite none receiving additional pembrolizumab cycles. These seven patients represented a mix of cancer types (two cohort B, three cohort C, one cohort D, one cohort E), and four of them displayed an OS of >18 months (range 19–27 months). Overall, the addition of Δ ctDNA_{C3} to C3 RECIST improved the accuracy of Cox models for OS (C statistic 0.62 versus 0.67, likelihood ratio test $P=0.02$).

Clearance of ctDNA during treatment identifies a highly favorable risk group. Having established the predictive value of Δ ctDNA_{C3} in patients treated with pembrolizumab, we asked whether dynamic changes throughout the course of treatment could add to the clinical utility of ctDNA-based monitoring. We measured ctDNA levels in all available plasma samples ($N=316$) from the entire cohort. ctDNA dynamic profiles were similar among patients with objective responses (complete response or partial response) and durable clinical benefit (stable disease for ≥ 6 cycles) (Fig. 5a). In these groups, ctDNA levels were stable or decreased over time in many patients, in contrast to the dramatic increases in ctDNA levels among many patients who did not derive clinical benefit.

Based on these differences, we evaluated the clinical outcomes among patients with distinct ctDNA dynamic profiles (Extended

Data Fig. 7). Among patients with at least two ctDNA measures, any rise in ctDNA levels during surveillance above baseline ($N=45$) was associated with rapid disease progression in most patients (Fig. 5b) and poor survival (median OS was 13.7 months, Fig. 6a). If ctDNA levels during surveillance remained below baseline but were still detectable ($N=16$), responses were mixed (Fig. 5b) and survival was marginally longer (median OS was 23.8 months, Fig. 6a).

If, however, ctDNA cleared during treatment (that is, became undetectable for at least one on-treatment time point), superior clinical outcomes were observed. Clearance of ctDNA occurred in 12 patients (Supplementary Table 8), with first clearance at C3 ($N=5$), C6 ($N=5$), C9 ($N=1$) or C12 ($N=1$) (Fig. 2). These 12 patients experienced prolonged objective responses (Fig. 5b) and 100% OS with a median of 25.4 (range 10.8–29.5) months of follow up beyond first clearance (Fig. 6a and Extended Data Fig. 8).

For patients with sustained ctDNA clearance and radiographic response during pembrolizumab, ctDNA clearance often preceded the radiographic response (Fig. 6b). For instance, a patient with malignant melanoma who cleared their ctDNA rapidly by C3 experienced gradual tumor regression over the course of 18 months. In a patient with SCCHN, ctDNA was cleared by 4 months whereas clinical response was not observed until 8 months on treatment. These examples illustrate the potential utility of ctDNA surveillance in patients with advanced solid tumors of diverse histologies who are treated with ICB.

Discussion

Biomarker-directed use of ICB is an important frontier in precision medicine^{1,7}. Despite the dramatic improvement in clinical

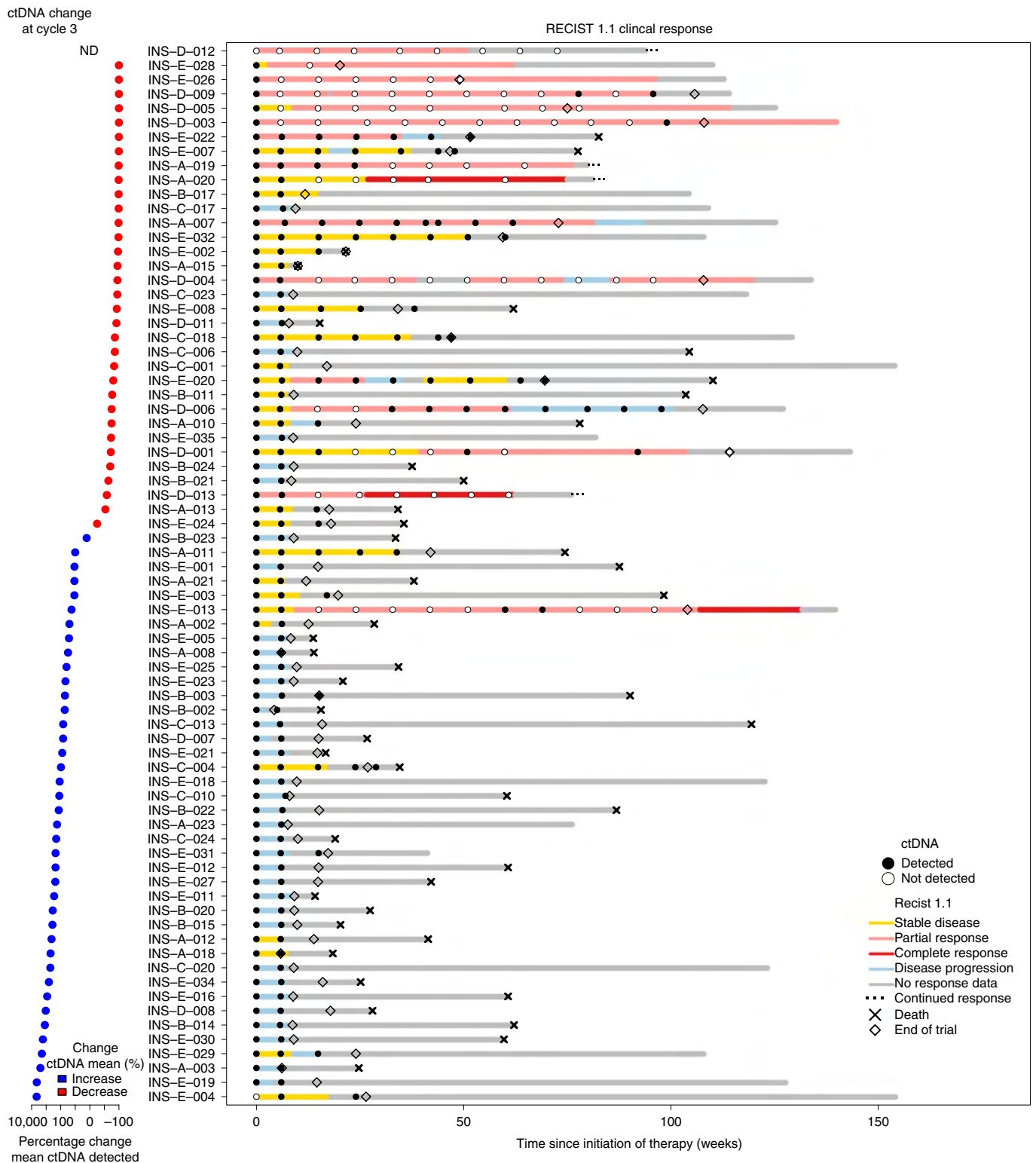


Fig. 2 | The change in ctDNA levels from baseline to C3, clinical response and survival. Patients with both baseline and on-treatment ctDNA levels are shown ($N = 74$ patients). Left, patients are ordered according to ctDNA change from baseline to C3 ($\Delta\text{ctDNA}_{\text{C3}}$). Right, swimmer plot showing clinical outcomes, duration on clinical trial and ctDNA detectability at assayed time points. The total length of each bar indicates the duration of survival from the time of first dose of pembrolizumab treatment. Line segments are colored according to the response criteria up to the time of RECIST1.1 assessment (endpoint of the color segment). When possible, continued RECIST1.1 assessment after end of trial was included. An open diamond symbol indicates the end of the trial. ND, no ctDNA detected at either baseline or C3.

outcomes in some cancer types, only a minority of patients with solid cancer will derive sustained response or meaningful clinical benefit. Putative biomarkers could provide clinical utility in

this setting by identifying patients most likely to benefit from ICB before or shortly after treatment initiation. Until now, few putative biomarkers have been clinically implemented agnostic to cancer

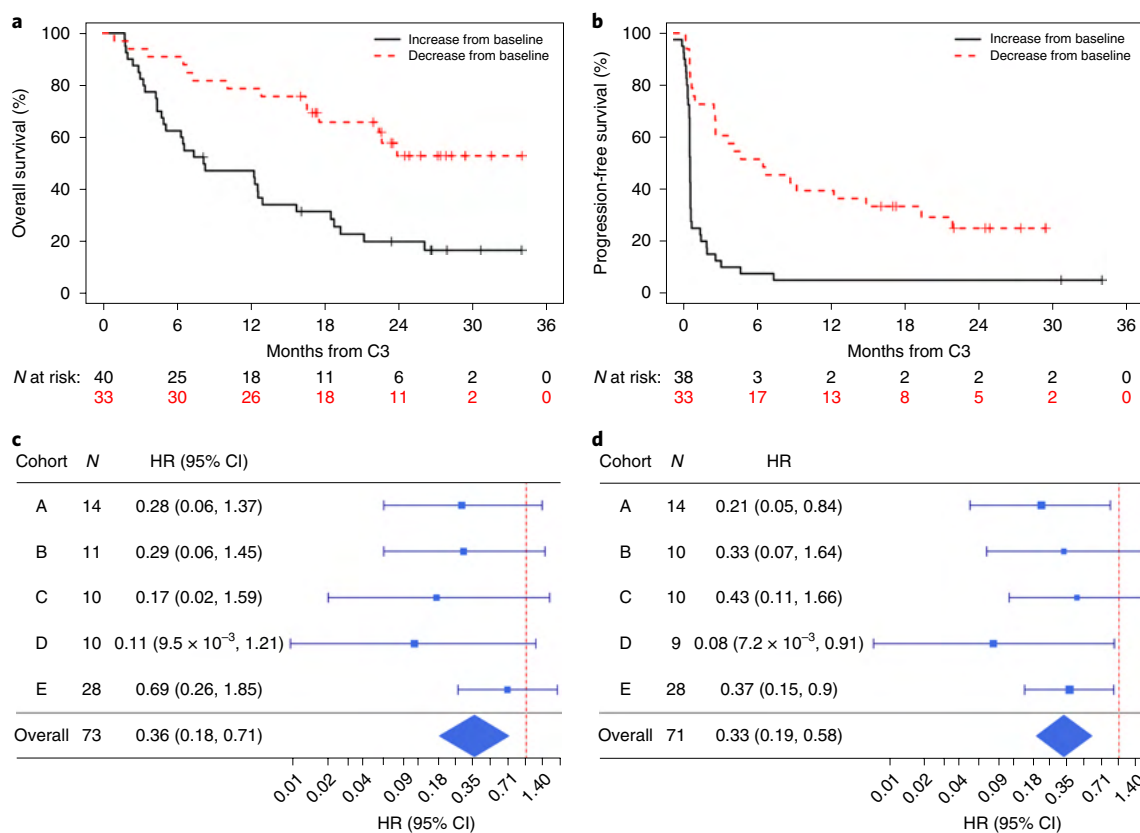


Fig. 3 | The change in ctDNA levels from baseline to C3 is strongly correlated with OS and PFS. a,b, Kaplan–Meier curves of OS (a) or PFS (b) among patients with both baseline and C3 ctDNA values stratified according to increase versus decrease of Δ ctDNA_{C3}. **c,d**, Forest plots depict the prognostic association of Δ ctDNA_{C3} with OS (c) or PFS (d) in the five subcohorts. The unadjusted hazard ratios (HR) (squares) and 95% confidence intervals (horizontal lines) are shown for each subcohort. The overall adjusted hazard ratios with 95% CIs for ctDNA_B after accounting for the cohorts are shown (diamonds). Vertical dotted line indicates the null hypothesis. N = 73 patients for OS analyses and N = 71 patients for PFS analyses due to two patients experiencing progression before C3.

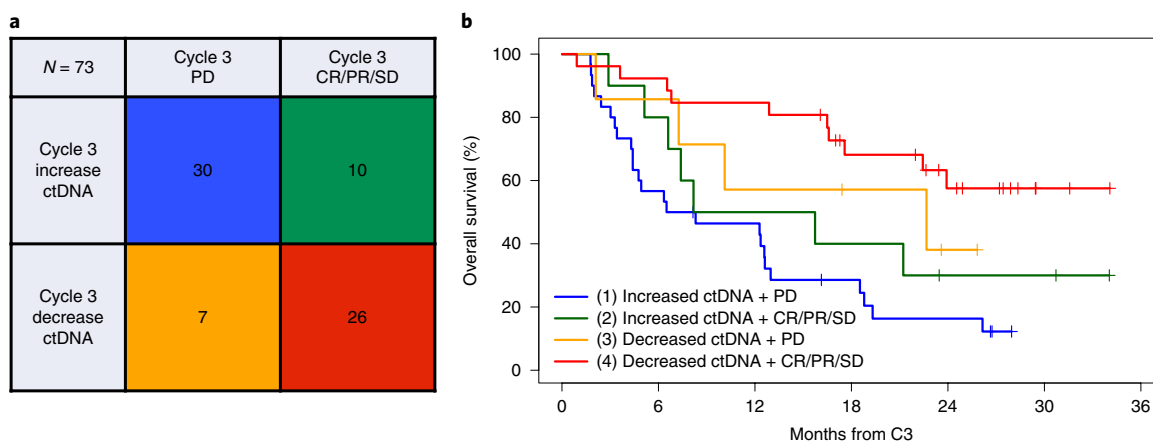


Fig. 4 | Risk groupings according to early clinical response and ctDNA kinetics. a, Cycle 3 RECIST groupings (columns) and Δ ctDNA_{C3} results (rows) are shown for 73 patients. **b**, Kaplan–Meier curve of OS among patients with at least two ctDNA measurements (N = 73 patients) stratified according to cycle 3 RECIST and Δ ctDNA_{C3} as in Fig. 4a. Two-sided log-rank P = 0.001. The magnitude of effect for group 1 (blue) versus group 3 (orange) comparison (aHR = 0.69) is similar to that of group 2 (green) versus group 4 (red) comparison (aHR = 0.62).

type. Tumor characteristics including TMB and PD-L1 have shown variable predictive value depending on cancer type. MSI-H phenotype identifies patients with favorable outcomes to ICB treatment² but is an uncommon feature in many cancer types including those enrolled in the INSPIRE trial.

Monitoring of ctDNA dynamics in patients treated by ICB could open the door to broader application of biomarker-directed ICB. ctDNA can be noninvasively accessed serially during treatment, with recent technological advances leading to improved availability and use. In this study, we focused on the clinical validity of ctDNA

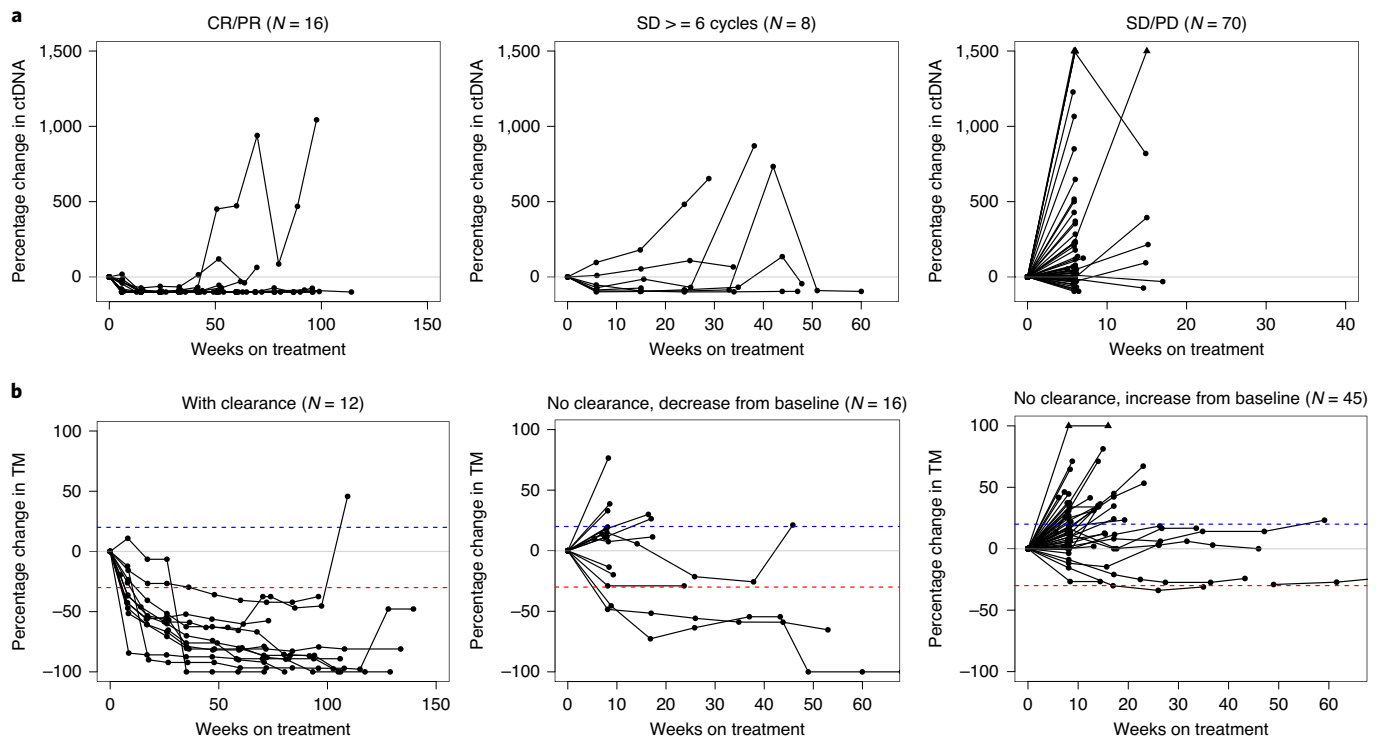


Fig. 5 | Objective clinical response to pembrolizumab is associated with ctDNA clearance. **a**, Serial ctDNA measurements in all patients ($N=94$ patients) grouped according to response groups: objective response (complete response (CR) or partial response (PR)); stable disease (SD) for ≥ 6 cycles; or all others (PD or SD < 6 cycles). Triangles indicate values off the displayed range of the y axis. **b**, RECIST tumor measurements (TM) during treatment grouped according to ctDNA dynamics (clearance at any on-treatment time point, no clearance with all on-treatment values below baseline, no clearance with any on-treatment value above baseline). Blue and red horizontal dotted lines indicate +20% and -30% change in tumor measurements, respectively.

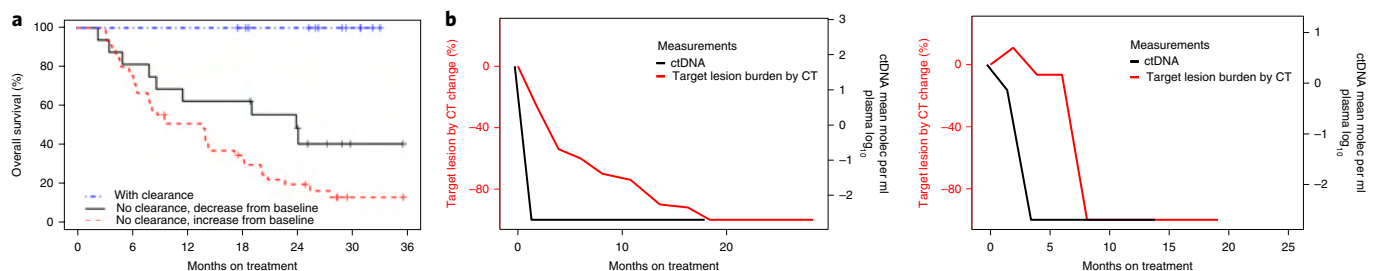


Fig. 6 | ctDNA clearance identifies patients with highly favorable survival. **a**, Kaplan-Meier curve of OS among patients with at least two ctDNA measurements ($N=73$ patients) stratified according to the clearance of ctDNA as in Fig. 5b. **b**, Examples of patients with ctDNA clearance followed by gradual and durable clinical response (RECIST1.1 target lesion tumor measurements). Left, INS-D-005 (malignant melanoma). Right, INS-A-020 (SCCHN). Source data for this figure is contained in the file Source data Fig. 6.

before and during ICB treatment as a prognostic, predictive and pharmacodynamic tool.

Although low baseline ctDNA levels were associated with favorable clinical outcomes in this multi-cohort study, the effect size was modest and partly confounded by tumor type. Patients with malignant melanoma, who may have a higher response rate to pembrolizumab than the other patients enrolled in INSPIRE, displayed the lowest average ctDNA levels. Of note, patients with TNBC were among those with the highest baseline ctDNA levels, which is consistent with other findings that ctDNA levels are higher in TNBC than other breast cancer subtypes²⁴. Baseline ctDNA levels were not strongly correlated with RECIST target lesion measurements (which does not incorporate measurements from nontarget lesions), suggesting that ctDNA could provide complementary information to RECIST.

The association of ctDNA levels with clinical outcomes was strongest and most consistent when considering on-treatment changes. In particular, an early reduction in ctDNA after two cycles of pembrolizumab treatment and on-treatment ctDNA clearance identified good prognosis subsets, independent of tumor type, TMB or PD-L1 status. Of note, patients with relatively low TMB were amenable to the highly targeted, personalized ctDNA assay. Thus, our findings demonstrate that serial ctDNA analysis using a bespoke assay could serve as a generalizable monitoring strategy for patients treated with ICB.

Results from this study also showed that an early rise in ctDNA levels was associated with a significantly higher rate of progression. Objective responses to ICB may be exceedingly rare in the setting of increasing ctDNA. This early ctDNA kinetic profile was complementary to clinical indices (RECIST) for identifying patients with

0% ORR and very poor survival, suggesting that these patients are very unlikely to benefit from continued treatment with single-agent ICB. Δ ctDNA_{C3} and C3 RECIST were discordant in 23% of cases, and the combination of these metrics was superior to C3 RECIST alone for predicting overall survival. Furthermore, on extended monitoring, a rise above the baseline ctDNA levels also identified patients unlikely to derive clinical benefit from continued treatment. Collectively, these patients may be ideal candidates for future clinical trials evaluating intensified or combination therapies.

Pseudoprogression early in the course of ICB treatment remains difficult to recognize with current clinical and radiological methods. As such, treatment beyond progression in patients who are clinically stable is common in patients treated with ICB. Although our study was not powered to specifically test the utility of ctDNA to discriminate true progression from pseudoprogression, we provide evidence that ctDNA could serve as a sensitive and reliable molecular predictor of ICB response. Further studies are warranted to examine whether ctDNA surveillance may facilitate timely therapeutic interventions in this setting to improve patient outcomes.

This study prospectively evaluated the value of ctDNA kinetics as a therapeutic biomarker during ICB treatment on a large scale. Previously, smaller studies and retrospective analyses have shown consistent findings that early on-treatment reduction in ctDNA levels identifies a favorable risk subset of patients treated with ICB^{13–21}. Due to the size and mature follow up of our study, we were able to evaluate the generalizability of our findings across the predefined INSPIRE cohorts (SCCHN, TNBC, HGSOC, malignant melanoma and MST). The observation that ctDNA clearance at any point during treatment was associated with long-term survival is provocative, underscoring the need for future prospective trials to rigorously test the potential clinical utility of ctDNA as a monitoring strategy for patients treated with ICB. Of note, 10 of 12 clearance events occurred by C6, but even delayed clearance at C9 and C12 appeared to confer favorable outcomes.

Additional strengths of our study include the homogeneous treatment regimen and the use of a ctDNA detection platform that is now commercially available to researchers and clinicians. The choice of a bespoke ctDNA assay allowed us to apply the test to all patients with available WES data, whereas a fixed panel approach may not have identified mutations in all patients. Using 16 mutations provided a higher degree of sensitivity than if only a single mutation had been selected. While we were not able to validate specific ctDNA thresholds in this study, to minimize overfitting and bias we dichotomized cohorts a priori according to median values or decrease versus increase. In our exploratory analysis, we found that deep reductions (for example, clearance) in ctDNA levels were most strongly associated with favorable prognosis. Future work could explore optimized cut-offs to further identify patients likely to experience long-term survival.

Limitations of this study include the lack of earlier on-treatment ctDNA assessment. Although ctDNA analysis was a planned objective of the INSPIRE study, the analysis was conducted with a research-use-only assay and was not done in real time. Moreover, 12 of 106 eligible patients enrolled in INSPIRE did not have the WES data required for bespoke ctDNA assay design, highlighting a practical barrier to implementing this strategy in a subset of patients when there are competing demands for tumor tissue²². While this study used fresh-frozen tumor biopsies in most patients, assay performance appeared to be similar in the subset of patients with only archival formalin-fixed paraffin-embedded (FFPE) tumor tissue available. We note that FFPE tumor tissues have also been used successfully with this bespoke platform in previous ctDNA surveillance studies^{23,25} with similar performance to fresh-frozen tissues²⁶. The method for calculating absolute ctDNA levels differed from previous reports using this assay^{23,25,26}; the calculation presented in this study, which is consistent with other published approaches²⁷,

provides a more accurate representation of the true amount of ctDNA in the patient's blood at the time of testing, particularly for low-value positive results and therefore supports optimal clinical interpretation (Extended Data Fig. 3). Additional validation of this approach will be needed to support clinical implementation.

In summary, the findings from this prospective study suggest broad clinical utility for ctDNA-based surveillance in patients treated with ICB. This is a noninvasive strategy to predict clinical benefit and long-term survival that could be generalizable across cancer types. Future interventional studies will be required to enable clinical decisions using ctDNA levels to guide ICB treatment.

Methods

Patients and study design. From 21 March 2016 to 9 May 2018, 106 patients with advanced solid tumors and available archived or baseline tumor tissue were enrolled in INSPIRE (NCT02644369)²². The study was approved by the Research Ethics Board at University Health Network. Adult patients provided informed consent and were accrued onto five parallel cohorts consisting of SCCHN (cohort A), TNBC (cohort B), HGSOC (cohort C), malignant melanoma (cohort D) and MST (cohort E). A listing of tumor histologies and patient frequencies represented within cohort E is provided in Supplementary Table 1. Patients were excluded if they had previously been treated with an anti-PD-1, anti-PD-L1 or anti-PD-L2 agent or if they had been treated with any anticancer monoclonal antibody therapy within 4 weeks. Treatment was conducted at Princess Margaret Cancer Centre with pembrolizumab 200 mg administered intravenously every 3 weeks. The study has completed enrollment but remains open for continued follow up of patients. The data collection cut-off date was 18 July 2019.

Clinical endpoints. OS was defined as time from first infusion to the date of death or the last date of follow up. Progress-free survival (PFS) was defined as time from first infusion to the date of progression, death or last follow up, whichever occurred first. Progression date was defined as the date of disease progression based on RECIST (v.1.1), or the date of clinical progression if the patient discontinued pembrolizumab due to clinical deterioration despite not meeting criteria for RECIST progression. ORR was defined as proportion of patients with complete response or partial response to pembrolizumab. CBR was defined as proportion of patients with complete response, partial response or stable disease lasting ≥ 6 cycles of pembrolizumab. Other endpoints of the INSPIRE trial include the change in genomics and immune landscapes, RNA expression correlates of treatment response, radiomic imaging analysis and tumor penetration of pembrolizumab as determined by mass spectrometry. Adverse events were monitored throughout the trial and graded in severity according to guidelines outlined in the NCI Common Terminology Criteria for Adverse Events v.4.03. After the end of treatment, each patient was followed for 30 d for adverse event monitoring (serious adverse events was collected for 90 d after the end of treatment).

Blood collection and processing. Peripheral blood plasma was collected at baseline and at the beginning of every three cycles during treatment. At each collection time point, 30 ml of peripheral blood was collected in EDTA tubes. Plasma was separated from the cell pellet within 2 h of collection and aliquoted for storage at -80°C . Cell-free DNA was purified from clarified plasma using the QIAamp Circulating Nucleic Acid Kit (Qiagen). Peripheral blood leukocyte (PBL) genomic DNA was extracted using the AllPrep DNA/RNA/miRNA Universal Extraction Kit (Qiagen). DNA and cell-free DNA was quantified using the Qubit dsDNA HS Assay Kit (ThermoFisher Scientific). All cell-free DNA samples were collected and processed by the Immune Monitoring Laboratory at the Princess Margaret Hospital (Toronto, Canada), and the Translational Genomics Laboratory at the Ontario Institute for Cancer Research (Toronto, Canada).

Tumor tissue processing. Fresh biopsy cores were enzymatically digested into single cell suspension using the gentle MACS Tissue Dissociation Kit (Miltenyi Biotec). Depending on availability, up to 25,000 cells were pelleted and flash frozen with dry ice and stored at -80°C . DNA and RNA were coextracted using the AllPrep DNA/RNA isolation kit (Qiagen). In the cases when insufficient genomic DNA was available from the biopsies, we acquired from the UHN Biobank FFPE tumor that had been obtained any time before trial enrollment. DNA and RNA were coextracted from macrodissected FFPE tissues using the AllPrep DNA/RNA FFPE extraction kit (Qiagen). Of 94 tumor tissues processed, 71 were from fresh-frozen tissues and 23 were FFPE. FFPE blocks of protocol-mandated baseline biopsy tissues were used for PD-L1 immunohistochemistry. Tissue sections of 4–5- μm thick were mounted on positively charged ProbeOn slides (QualTek) and stained with anti-PD-L1 (clone 22C3). Details of the PD-L1 staining and scoring procedures using modified proportion score were published previously²².

WES. Illumina-compatible sequencing libraries were constructed from tumor and matched PBL genomic DNA. Exome hybrid capture was conducted using the Agilent SureSelectXT Human All Exon v.5 +UTR probe set and reagents (Agilent).

Exome libraries were sequenced with paired-end 125 bp reads on the Illumina HiSeq2000 or HiSeq2500 platform (Illumina) to a median depth of 250× for tumor samples and 50× for PBL samples. Sequence data was aligned to human reference genome version GRCh38 using Burrows–Wheeler Alignment tool (v.0.7.12). Somatic mutations were detected for each tumor and PBL data pair using VarScan2 (ref. 28), GATK MuTect2 and HaplotypeCaller²⁹, MuTect³⁰ and Vardict³¹. Tumor mutation burden was calculated as the total number of nonsynonymous mutations detected in more than two out of five mutation callers for each sample. MSI status was determined for each tumor and normal using mSINGS³² with provided list of microsatellite genomic loci mapped to the GRCh38 reference using the UCSC LiftOver utility (<https://genome.ucsc.edu/cgi-bin/hgLiftOver>) and default parameters and detection cut-off. Sequencing and data processing were completed by the Princess Margaret Genome Centre (Toronto, Canada) and the Translational Genomics Laboratory at the Ontario Institute for Cancer Research (Toronto, Canada).

Personalized ctDNA assays. Design and application of personalized ctDNA (bespoke, multiplex-PCR, next-generation sequencing) assays was conducted with blinding to clinical data by Natera. Paired tumor and PBL WES data were used to identify tumor-specific somatic mutations for each patient and clonality was estimated as described previously³³. Multiplex-PCR primer pairs targeting 16 highly ranked tumor-specific variants were designed as previously described^{23,25,26}. The primer sequences for each variant are from the Signatera assay and are proprietary of Natera. Somatic small nucleotide variants present in the tumor but absent in the germline were used to select the 16 targets, with prioritization based on multiple factors, including the observed variant allele frequency in the tumor tissue and the associated background noise profile in the plasma. This prioritized list of variants was then used to design PCR amplicons based on optimized design parameters, ensuring uniqueness in the human genome, amplicon efficiency and primer interaction. Next, multiplexed targeted PCR was conducted followed by amplicon deep sequencing on an Illumina platform. A sample was considered ctDNA positive when ≥ 2 out of the 16 selected target mutations were present at above a predefined threshold^{23,25,26}. Details of the analytical validation of the assay were previously described²³. Variant allele frequencies were determined for each of the 16 target mutations. Absolute ctDNA levels (MTM per ml) in the plasma were determined by normalizing variant allele frequencies by the plasma volume used for each sample. At each time point, MTM per ml was calculated from all 16 tested targets (including undetected targets); this provides a more accurate representation of the true amount of ctDNA than using only the detected targets to calculate the mean (Extended Data Fig. 3). The change in ctDNA from baseline to C3 (Δ ctDNA_{C3}) was defined as the percentage change in absolute ctDNA levels in plasma at cycle 3 since baseline. ctDNA clearance was defined as ctDNA of zero at any time point.

Statistics and reproducibility. To minimize bias, ctDNA measurements were conducted with blinding to clinical data, and patient treatment and clinical data collection were conducted with blinding to ctDNA measurements. A statistical analysis plan was designed before data analysis. The primary outcome was PFS, and OS was the secondary endpoint. In the primary analysis, data from all five subcohorts were combined and analyzed as a single cohort for evaluation. We hypothesized that the presence of ctDNA at the baseline and post-treatment would be associated with decreased PFS and OS. No statistical method was used to predetermine sample size. There was no randomization as part of the study design. No data were excluded from the analyses. Descriptive statistics were used to summarize patients and clinical characteristics, with median and range for continuous variables and frequency and percentage for categorical variables. Swimmer plot was provided to visualize clinical response and Δ ctDNA_{C3} change for each patient. The Wilcoxon rank sum test was used to compare the number of mutations detected in baseline cell-free DNA samples according to whether the bespoke assay design was conducted from FFPE versus fresh-frozen tumor exomes. Correlation between the measurements of ctDNA_B, Δ ctDNA_{C3}, baseline target lesion size, PD-L1 immunohistochemistry and TMB were calculated using Spearman correlation coefficients. Differences in TMB and ctDNA values between cohorts were measured by the Kruskal–Wallis test. To assess the effect of ctDNA_B on OS and PFS, Kaplan–Meier curves were used to compare the performance between those with a ctDNA_B above and below median. Cox proportional hazards regression models (univariate, or bivariable with adjusting for cohort) were used to assess the impact of ctDNA_B on OS and PFS. Fisher's exact test was used to assess the association of ctDNA_B with ORR and CBR. Forest plot was used to visualize the estimated hazard ratios by cohort. Similar analyses were carried out to assess the impact of Δ ctDNA_{C3} on the clinical outcomes (OS, PFS, ORR and CBR) among patients with both baseline and C3 ctDNA data available. Univariate analyses were used to select a priori variables for inclusion in the multivariable analyses. Multivariable Cox models were used to assess the impact of Δ ctDNA_{C3} on OS and PFS, while adjusting for cohort, PD-L1 immunohistochemistry and TMB. Kaplan–Meier curves with log-rank test and Cox models with C statistic and likelihood ratio test were used to evaluate the impact of Δ ctDNA_{C3} and cycle 3 RECIST on OS. Multivariable logistic regression models were used to assess the impact of Δ ctDNA_{C3} on ORR and CBR respectively, while adjusting

for PD-L1 or TMB. An exploratory analysis comparing OS between those with and without ctDNA clearance was carried out. All tests were two-sided. Results were considered statistically significant if the *P* value was ≤ 0.05 . All statistical analyses were performed using R (R Foundation for Statistical Computing, <https://www.R-project.org/>). Further information on research design is available in the Nature Research Reporting Summary linked to this article.

Reporting Summary. Further information on research design is available in the Nature Research Reporting Summary linked to this article.

Data availability

Anonymized WES data of tumor and match normals are available with controlled access approval through the European Genome-Phenome Archive under accession number EGAS00001003280. Source data for Figs. 1–6 can be found in Source data Figs. 1–6 files, and Source data for Extended Data Fig. 2–8 can be found in Source data Extended Data Fig. 2–8 files. The supporting variant level data for all figures are available in Supplementary Table 4. All other data supporting the findings of this study are available from the corresponding author on reasonable request. Source data are provided with this paper.

Code availability

Code necessary to reproduce the core analyses are available without restrictions at <https://github.com/pughlab/inspire-ctdna>.

Received: 7 March 2020; Accepted: 26 June 2020;

References

- Bedognetti, D. et al. Toward a comprehensive view of cancer immune responsiveness: a synopsis from the SITC workshop. *J. Immunother. Cancer* **7**, 131 (2019).
- Hause, R. J., Pritchard, C. C., Shendure, J. & Salipante, S. J. Classification and characterization of microsatellite instability across 18 cancer types. *Nat. Med.* **22**, 1342–1350 (2016).
- Jenkins, R. W., Thummalapalli, R., Carter, J., Canadas, I. & Barbie, D. A. Molecular and genomic determinants of response to immune checkpoint inhibition in cancer. *Annu. Rev. Med.* **69**, 333–347 (2018).
- Rizvi, N. A. et al. Cancer immunology. Mutational landscape determines sensitivity to PD-1 blockade in non-small cell lung cancer. *Science* **348**, 124–128 (2015).
- Snyder, A. et al. Genetic basis for clinical response to CTLA-4 blockade in melanoma. *N. Engl. J. Med.* **371**, 2189–2199 (2014).
- Tumeh, P. C. et al. PD-1 blockade induces responses by inhibiting adaptive immune resistance. *Nature* **515**, 568–571 (2014).
- Gibney, G. T., Weiner, L. M. & Atkins, M. B. Predictive biomarkers for checkpoint inhibitor-based immunotherapy. *Lancet Oncol.* **17**, e542–e551 (2016).
- Eisenhauer, E. A. et al. New response evaluation criteria in solid tumours: revised RECIST guideline (version 1.1). *Eur. J. Cancer* **45**, 228–247 (2009).
- Wolchok, J. D. et al. Guidelines for the evaluation of immune therapy activity in solid tumors: immune-related response criteria. *Clin. Cancer Res.* **15**, 7412–7420 (2009).
- Ribas, A., Chmielowski, B. & Glaspy, J. A. Do we need a different set of response assessment criteria for tumor immunotherapy? *Clin. Cancer Res.* **15**, 7116–7118 (2009).
- Corcoran, R. B. & Chabner, B. A. Application of cell-free DNA analysis to cancer treatment. *N. Engl. J. Med.* **379**, 1754–1765 (2018).
- Cabel, L. et al. Clinical potential of circulating tumour DNA in patients receiving anticancer immunotherapy. *Nat. Rev. Clin. Oncol.* **15**, 639–650 (2018).
- Anagnostou, V. et al. Dynamics of tumor and immune responses during immune checkpoint blockade in non-small cell lung cancer. *Cancer Res.* **79**, 1214–1225 (2019).
- Cabel, L. et al. Circulating tumor DNA changes for early monitoring of anti-PD1 immunotherapy: a proof-of-concept study. *Ann. Oncol.* **28**, 1996–2001 (2017).
- Giroux Leprieur, E. et al. Circulating tumor DNA evaluated by Next-Generation Sequencing is predictive of tumor response and prolonged clinical benefit with nivolumab in advanced non-small cell lung cancer. *Oncotarget* **7**, e1424675 (2018).
- Goldberg, S. B. et al. Early assessment of lung cancer immunotherapy response via circulating tumor DNA. *Clin. Cancer Res.* **24**, 1872–1880 (2018).
- Gray, E. S. et al. Circulating tumor DNA to monitor treatment response and detect acquired resistance in patients with metastatic melanoma. *Oncotarget* **6**, 42008–42018 (2015).
- Lee, J. H. et al. Circulating tumour DNA predicts response to anti-PD1 antibodies in metastatic melanoma. *Ann. Oncol.* **28**, 1130–1136 (2017).

19. Lee, J. H. et al. Association between circulating tumor DNA and pseudoprogression in patients with metastatic melanoma treated with anti-programmed cell death 1 antibodies. *JAMA Oncol.* **4**, 717–721 (2018).
20. Raja, R. et al. Early reduction in ctDNA predicts survival in patients with lung and bladder cancer treated with durvalumab. *Clin. Cancer Res.* **24**, 6212–6222 (2018).
21. Moding, E. J. et al. Circulating tumor DNA dynamics predict benefit from consolidation immunotherapy in locally advanced non-small-cell lung cancer. *Nat. Cancer* **1**, 176–183 (2020).
22. Clouthier, D. L. et al. An interim report on the investigator-initiated phase 2 study of pembrolizumab immunological response evaluation (INSPIRE). *J. Immunother. Cancer* **7**, 72 (2019).
23. Coombes, R. C. et al. Personalized detection of circulating tumor DNA antedates breast cancer metastatic recurrence. *Clin. Cancer Res.* **25**, 4255–4263 (2019).
24. Magbanua, M. J. M. et al. Circulating tumor DNA in neoadjuvant treated breast cancer reflects response and survival. Preprint at *medRxiv* <https://doi.org/10.1101/2020.02.03.20019760> (2020).
25. Christensen, E. et al. Early detection of metastatic relapse and monitoring of therapeutic efficacy by ultra-deep sequencing of plasma cell-free DNA in patients with urothelial bladder carcinoma. *J. Clin. Oncol.* **37**, 1547–1557 (2019).
26. Reinert, T. et al. Analysis of plasma cell-free DNA by ultradeep sequencing in patients with stages I to III colorectal cancer. *JAMA Oncol.* **5**, 1124–1131 (2019).
27. Newman, A. M. et al. Integrated digital error suppression for improved detection of circulating tumor DNA. *Nat. Biotechnol.* **34**, 547–555 (2016).
28. Koboldt, D. C. et al. VarScan 2: somatic mutation and copy number alteration discovery in cancer by exome sequencing. *Genome Res.* **22**, 568–576 (2012).
29. McKenna, A. et al. The Genome Analysis Toolkit: a MapReduce framework for analyzing next-generation DNA sequencing data. *Genome Res.* **20**, 1297–1303 (2010).
30. Cibulskis, K. et al. Sensitive detection of somatic point mutations in impure and heterogeneous cancer samples. *Nat. Biotechnol.* **31**, 213–219 (2013).
31. Lai, Z. et al. VarDict: a novel and versatile variant caller for next-generation sequencing in cancer research. *Nucleic Acids Res.* **44**, e108 (2016).
32. Salipante, S. J., Scroggins, S. M., Hampel, H. L., Turner, E. H. & Pritchard, C. C. Microsatellite instability detection by next generation sequencing. *Clin. Chem.* **60**, 1192–1199 (2014).
33. McGranahan, N. et al. Clonal status of actionable driver events and the timing of mutational processes in cancer evolution. *Sci. Transl. Med.* **7**, 283ra254 (2015).

Acknowledgements

Major funding support for the project was made possible by the Princess Margaret Cancer Foundation, Ontario Institute for Cancer Research and Terry Fox Research Institute. We thank Merck for contributing the study drug for the clinical trial. S.V.B. and T.J.P. were supported by the Gattuso-Slaight Personalized Cancer Medicine Fund. S.Y.C.Y. was supported in part by the University of Toronto Medical Biophysics OSOTF Excellence Award. M.A.J.I. was supported in part by a fellowship through the BMO Chair in Precision Cancer Genomics. L.L.S. holds the BMO Chair in Precision Cancer Genomics. T.J.P. holds the Canada Research Chair in Translational Genomics and is supported by a Senior Investigator Award from the Ontario Institute for Cancer Research. We are grateful to R. Salari, H.-T. Wu and S. Dashner for their technical support and insightful discussions of the project. We gratefully acknowledge the

individuals from the Princess Margaret Tumour Immunotherapy Program (<https://www.pm-tumourimmunotherapyprogram.ca/>), including the immune monitoring (M. Butler, D. Gray, V. Sotov and D. Liu) and tissue correlatives (V. Speers, A. Giesler and S. Hakgor) teams. We thank the staff of the Princess Margaret Genomics Centre (<https://www.pmggenomics.ca>), Bioinformatics and High-Performance Computing Core, and PM-OICR Translational Genomics Laboratory (<https://labs.oicr.on.ca/translational-genomics-laboratory>) for their expertise in generating the sequencing data used in this study. Additional infrastructure support from the Canada Foundation for Innovation, Leaders Opportunity Fund (32383); Ontario Ministry of Research and Innovation, Ontario Research Fund Small Infrastructure Program and Ontario Institute for Cancer Research (<https://genomics.oicr.on.ca>).

Author contributions

S.V.B., L.L.S. and T.J.P. conceived the study. S.V.B., P.S.O., L.L.S. and T.J.P. secured funding. S.Y.C.Y. performed data analysis. M.A.J.I. reviewed the clinical data and performed data analysis. A.R.H., P.L.B., S.L., A.S., A.A.R. and L.L.S. accrued patients and supervised biospecimen sample collection. T.J.P., P.S.O., D.L.C. and D.T. supervised biospecimen sample processing by S.Y.C.Y., S.C.L., Y.H., I.C., K.M. and J.E. W.X. and Z.L. performed statistical analysis. S.S., M.L., B.Z., P.B., H.S. and A.A. conducted the ctDNA assays and provided technical expertise and scientific feedback. S.V.B., S.Y.C.Y., L.L.S., W.X., Z.L., D.T. and T.J.P. wrote the manuscript. All authors discussed the results and implications and commented on the manuscript at all stages.

Competing interests

S.V.B. provides consultation for Bristol-Myers Squibb, receives research support from Nektar Therapeutics and is a coinventor on a patent application relating to circulating tumor DNA mutation detection technology (PCT/US2014/02502, licensed to Roche Molecular Diagnostics) and on a patent application relating to ctDNA methylation analysis technology (PCT/CA2018/000203). L.L.S. provides consultation for Merck (compensated), Pfizer (compensated), Celgene (compensated), AstraZeneca (compensated), Morphosys (compensated), Roche (compensated), GeneSeq (compensated), Loxo (compensated), Oncorus (compensated), Symphogen (compensated), Seattle Genetics (compensated), GlaxoSmithKline (compensated), Voronoi (compensated), Treadwell Therapeutics (compensated), Arvinas (compensated), Tessa (compensated), Navire (compensated); receives research support (institutional) from Novartis, Bristol-Myers Squibb, Pfizer, Boehringer-Ingelheim, GlaxoSmithKline, Roche/Genentech, Karyopharm, AstraZeneca/Medimmune, Merck, Celgene, Astellas, Bayer, Abbvie, Amgen, Symphogen, Intensity Therapeutics, Mirati, Shattucks and Avid; and is a stockholder in Agios (spouse) and Treadwell Therapeutics (spouse). S.S., M.L., P.B., B.Z., H.S. and A.A. are employees of Natera, Inc. T.J.P. provides consultation for Merck, Chrysalis Biomedical Advisors and the Canadian Pension Plan Investment Board, and receives research support from Roche.

Additional information

Extended data is available for this paper at <https://doi.org/10.1038/s43018-020-0096-5>.

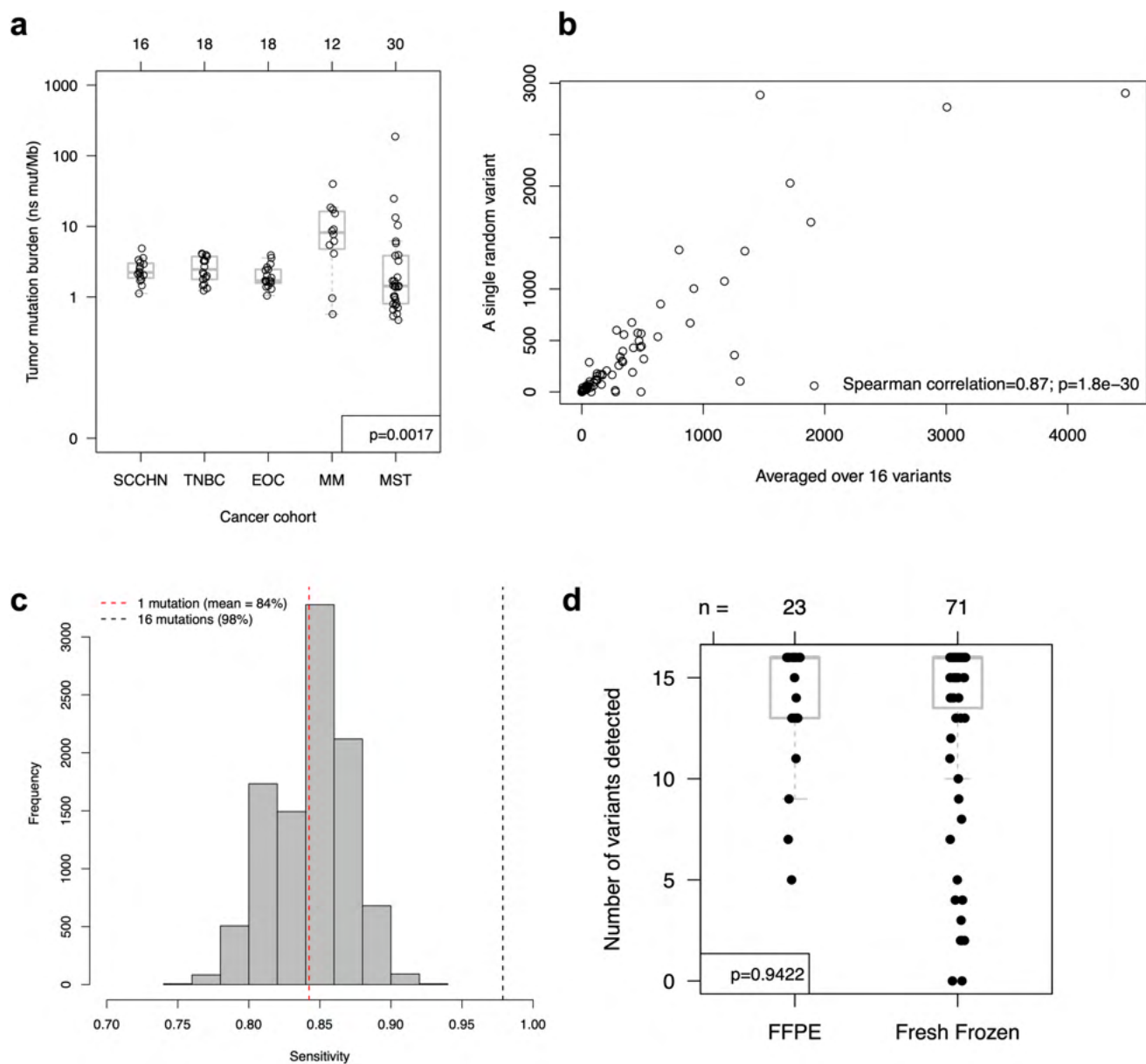
Supplementary information is available for this paper at <https://doi.org/10.1038/s43018-020-0096-5>.

Correspondence and requests for materials should be addressed to L.L.S. or T.J.P.

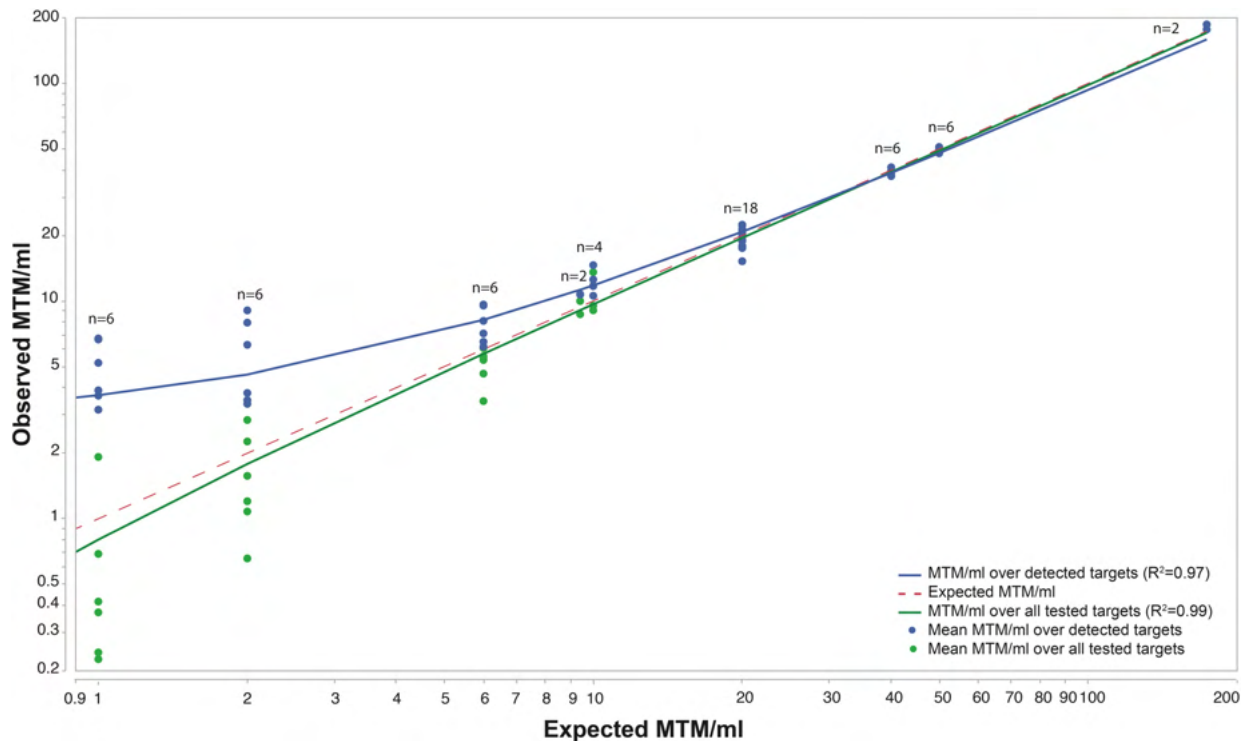
Reprints and permissions information is available at www.nature.com/reprints.

Publisher's note Springer Nature remains neutral with regard to jurisdictional claims in published maps and institutional affiliations.

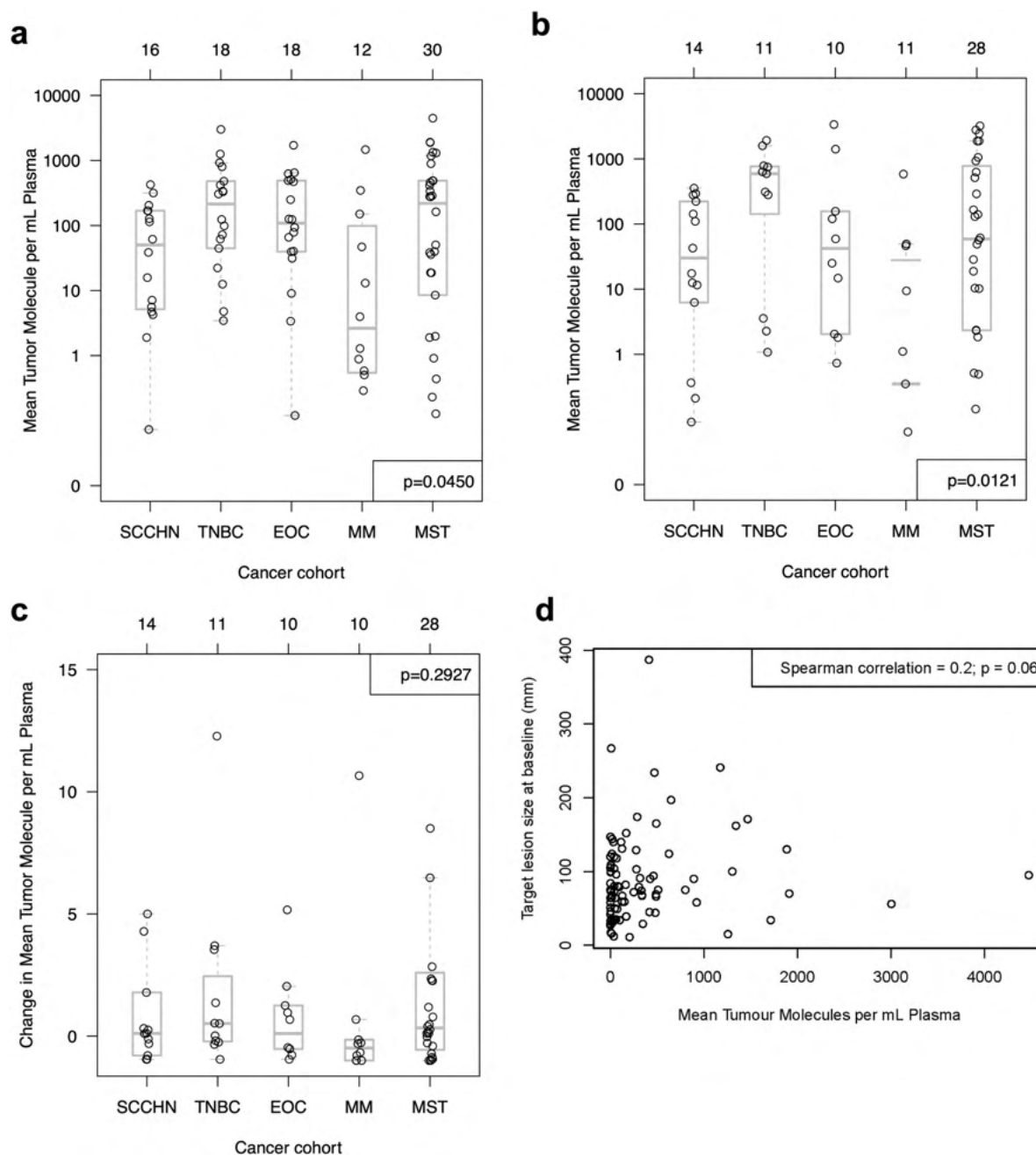
© The Author(s), under exclusive licence to Springer Nature America, Inc. 2020



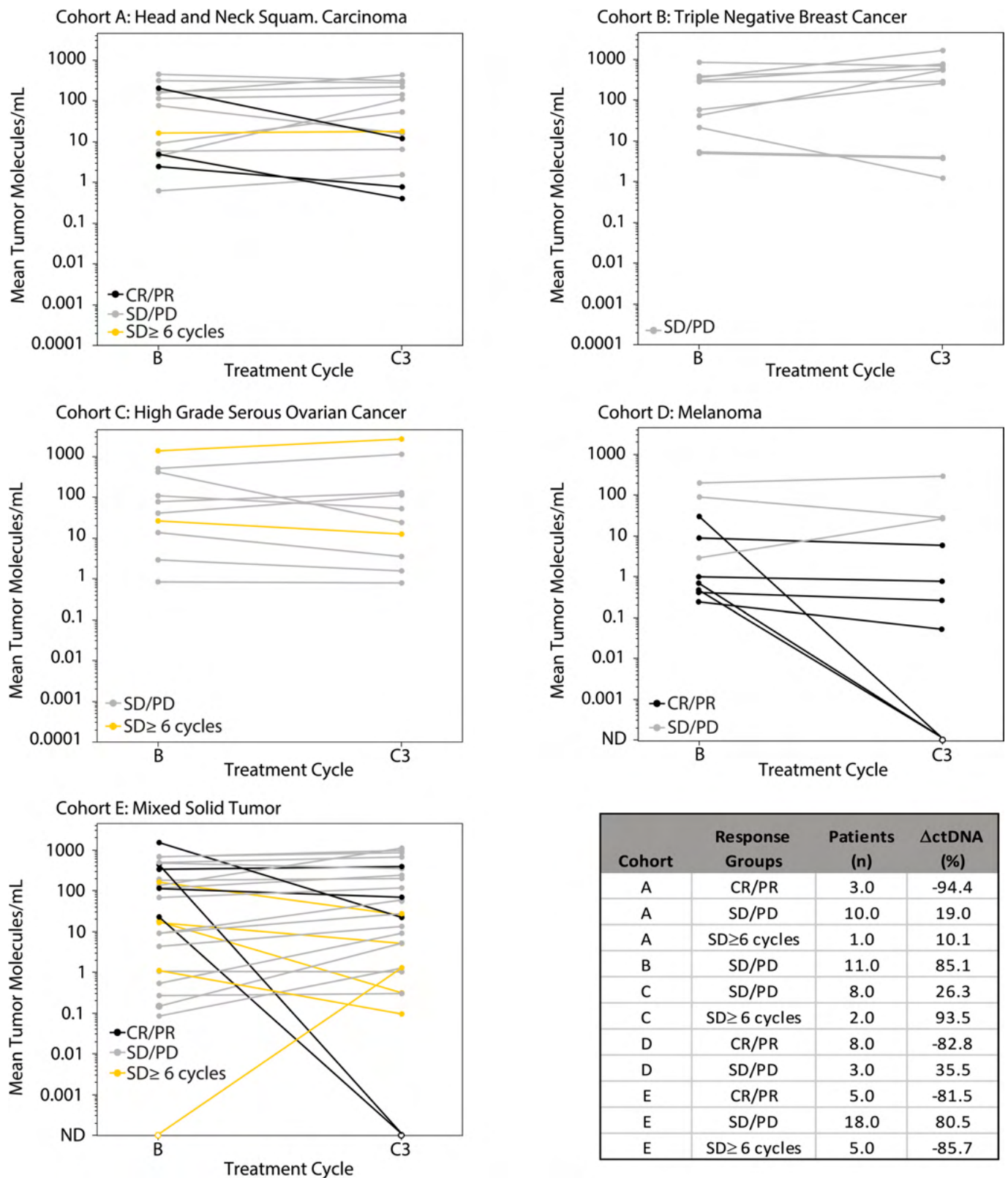
Extended Data Fig. 2 | Factors affecting somatic mutation detection in tumor tissue and plasma cell-free DNA. **a**, Somatic mutation burden per patient are grouped by INSPIRE cancer cohorts: Squamous cell cancer of head and neck (SCCHN, cohort A), triple negative breast cancer (TNBC, cohort B), high grade serous ovarian cancer (HGSOC, cohort C), malignant melanoma (MM, cohort D), and mixed solid tumors (MST, cohort E). The N (patients) for each group is shown in the top axis. Two-sided Kruskal-Wallis test p-value is shown. **b, c**, Comparison of 16 mutations vs 1 mutation from sequencing data for detecting ctDNA. To evaluate the impact of measuring 16 mutations on the likelihood of detecting ctDNA, we randomly selected one of the 16 mutations from each of the 94 baseline cell-free DNA samples and repeated this with 10,000 iterations. **(b)** An example of one of the 10,000 iteration shows that ctDNA levels (MTM/mL) are correlated (Spearman $R = 0.87$) among $N = 94$ baseline cell-free DNA samples. Two-sided Spearman correlation test p-value is shown. **(c)** Histogram of the detection likelihood (sensitivity for ctDNA) from 94 baseline cell-free DNA samples when using a randomly selected single mutation ($N = 10,000$ iterations). The mean sensitivity (red dashed line) is 84%. The sensitivity using all 16 mutations (black dashed line) is 98%. **d**, Influence of tumor tissue source used for bespoke assay design on detectability of ctDNA. The number of detected variants in baseline cell-free DNA samples are shown according to whether the bespoke assay design was conducted from FFPE vs fresh-frozen tumor exomes. Total number of samples in each group shown on the top axis. Two-sided Wilcoxon rank sum test p-value is shown. Box plots represent the median, upper and lower quartiles of each distribution with whiskers showing the limits of the distribution (1.5 times the interquartile range).



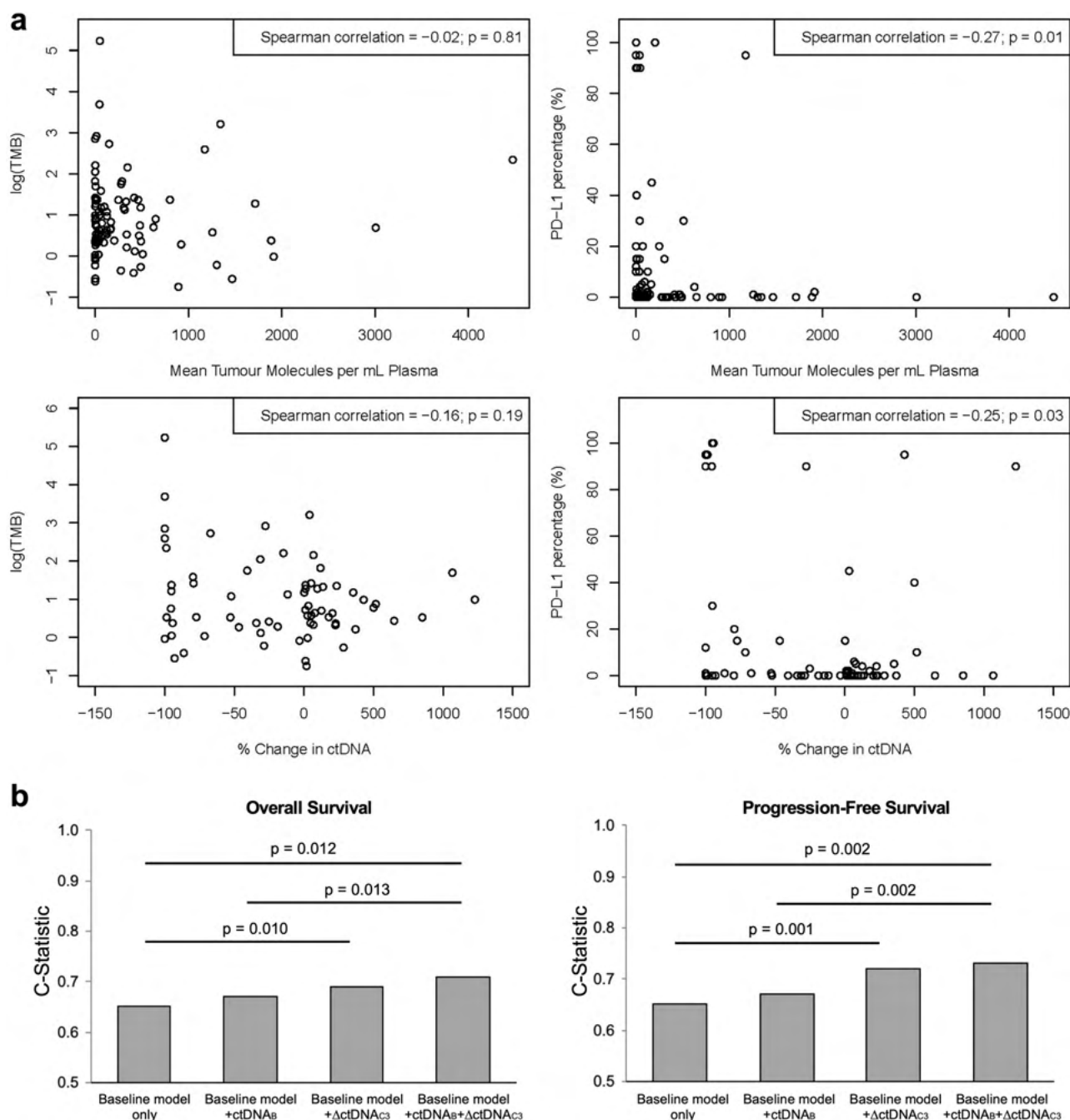
Extended Data Fig. 3 | Rationale for calculation of absolute ctDNA levels from multiple mutation targets. Analytical validation of the ctDNA quantification approach was conducted using Sereq ctDNA Mutation Mix v2 (SeraCare, Milford, MA, USA) at various concentrations. For a given sample containing 16 target mutations, the mean tumor molecules per mL of plasma (MTM/mL) was calculated using two approaches (y-axis) and compared to known concentrations (x-axis). The blue data points represent the per-sample measurements of mean MTM/mL calculated over detected targets (slope=0.86), while the green data points represent the per-sample measurements of mean MTM/mL calculated over all 16 tested targets (slope=0.98). The red (X=Y) dashed line illustrates the ideal (expected) scenario in which the calculated experimental ctDNA levels are equal to the expected MTM/mL. The numbers of technical replicates at each concentration are shown (n = 2-18). In addition, all 10 negative control samples had no detected mutations (not shown). Pearson correlation coefficients (R^2) are shown. This analytical comparison indicates that mean MTM/mL calculated over all tested targets provides a more accurate representation of the true amount of ctDNA, particularly at low levels of ctDNA.



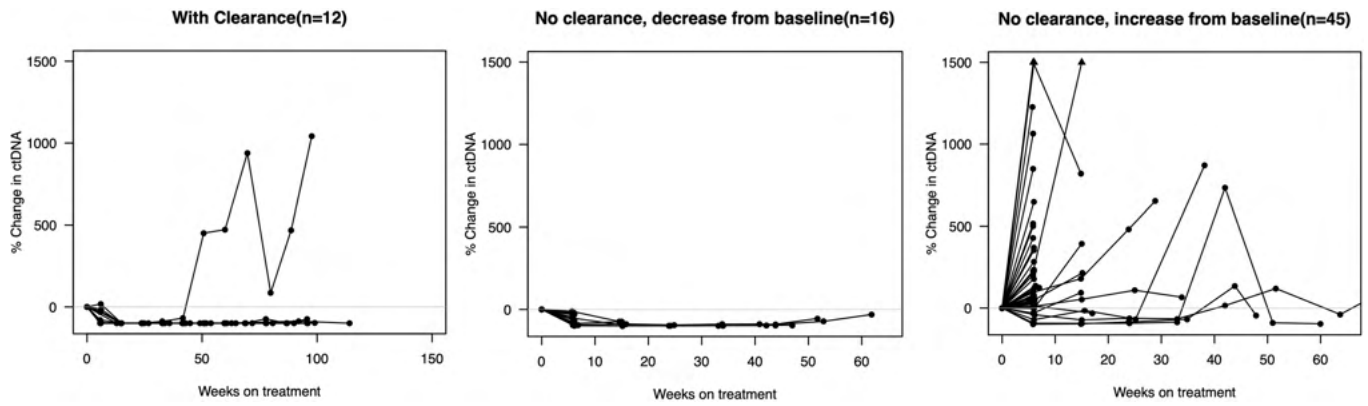
Extended Data Fig. 4 | ctDNA levels in the INSPIRE sub-cohorts and correlation with RECIST tumor measurements. ctDNA levels (MTM/mL) at baseline **a**, and at cycle 3 **b**, as well as the fold-change in ctDNA levels from baseline to cycle 3 (Δ ctDNA_{c3}) **c**, are shown for each of the sub-cohorts: Squamous cell cancer of head and neck (SCCHN, cohort A), triple negative breast cancer (TNBC, cohort B), high grade serous ovarian cancer (HGSO, cohort C), malignant melanoma (MM, cohort D), and mixed solid tumors (MST, cohort E). Box plots represent the median, upper and lower quartiles of each distribution with whiskers showing the limits of the distribution (1.5 times the interquartile range). The N (patients) for each group is shown in the top axis. Two-sided Kruskal-Wallis test p-values are shown for **(a-c)**. **d**, Relationship between ctDNA₈ and RECIST 1.1 target lesion sum of tumor measurements (N = 94 patients). Scatter plot with Spearman correlation coefficient (R) and two-sided p-value are shown. The poor correlation in this diverse cohort of advanced cancers suggests that ctDNA may provide complementary information to RECIST tumor measurements. Of note, RECIST target lesion sum of tumor measurements does not incorporate measurements from non-target lesions.



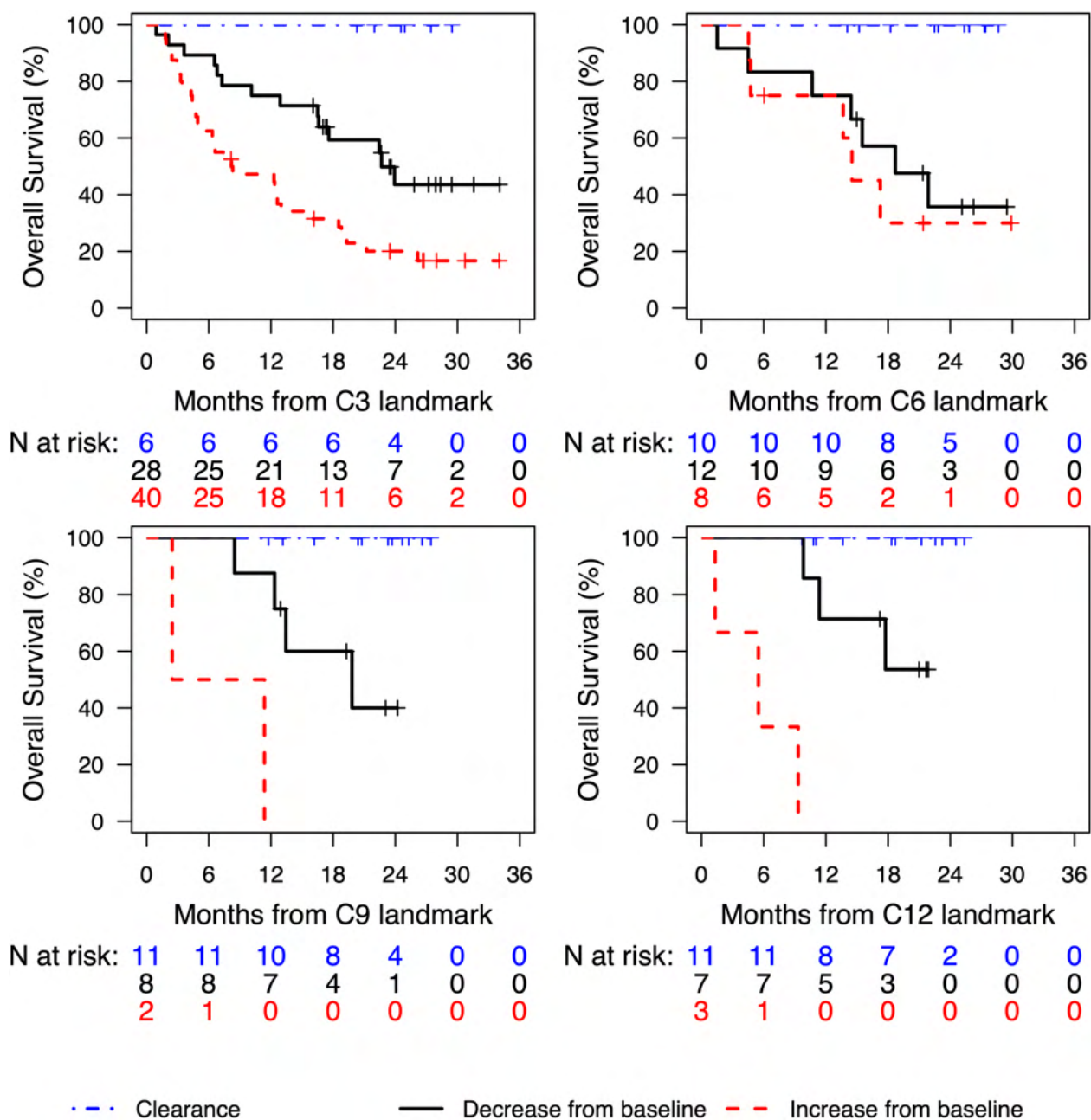
Extended Data Fig. 5 | $\Delta\text{ctDNA}_{\text{C3}}$ for the INSPIRE sub-cohorts. Clinical response is indicated by line color. The inset table summarizes $\Delta\text{ctDNA}_{\text{C3}}$ values among patients with distinct clinical responses in each sub-cohort. Closed circles indicate ctDNA positive samples and open circles indicate ctDNA negative samples; SD, stable disease; CR, complete response; PR, partial response; PD, progressive disease; B, baseline; C3, cycle 3; ND, not detected (below detection threshold).



Extended Data Fig. 6 | Relationship between ctDNA, biomarkers, and prognosis. **a**, Relationship between ctDNA metrics (ctDNA_B or ΔctDNA_{C3}) and other candidate biomarkers (PD-L1 or TMB). Scatter plots with Spearman correlation coefficients (R) and p-values are shown. Top row: N = 94 patients with both ctDNA_B and TMB levels; N = 93 patients with both ctDNA_B and PD-L1 levels. Bottom row: N = 72 patients with ΔctDNA_{C3}, TMB, and PD-L1 levels. **b**, Performance of multivariable Cox models incorporating ctDNA metrics (ctDNA_B and/or ΔctDNA_{C3}). Multivariable Cox models for OS (left) or PFS (right) were generated. The baseline model incorporates cohort, PD-L1, and TMB. C-statistic is plotted for each model. Statistically significant differences (two-sided likelihood ratio test) are indicated.



Extended Data Fig. 7 | Definitions of ctDNA dynamic profiles. Serial ctDNA measurements in patients grouped according to ctDNA dynamics (clearance at any time point, no clearance with all on-treatment values below baseline, no clearance with any on-treatment value above baseline). Triangles indicate values off the displayed range of the y-axis.



Extended Data Fig. 8 | Landmark analyses of ctDNA clearance. Kaplan-Meier curves of OS among patients classified as one of 3 groups (Clearance; Decrease from baseline; Increase from baseline) based on ctDNA at each indicated landmark (that is, C3, C6, C9, or C12).

Reporting Summary

Nature Research wishes to improve the reproducibility of the work that we publish. This form provides structure for consistency and transparency in reporting. For further information on Nature Research policies, see [Authors & Referees](#) and the [Editorial Policy Checklist](#).

Statistics

For all statistical analyses, confirm that the following items are present in the figure legend, table legend, main text, or Methods section.

n/a Confirmed

- The exact sample size (n) for each experimental group/condition, given as a discrete number and unit of measurement
- A statement on whether measurements were taken from distinct samples or whether the same sample was measured repeatedly
- The statistical test(s) used AND whether they are one- or two-sided
Only common tests should be described solely by name; describe more complex techniques in the Methods section.
- A description of all covariates tested
- A description of any assumptions or corrections, such as tests of normality and adjustment for multiple comparisons
- A full description of the statistical parameters including central tendency (e.g. means) or other basic estimates (e.g. regression coefficient) AND variation (e.g. standard deviation) or associated estimates of uncertainty (e.g. confidence intervals)
- For null hypothesis testing, the test statistic (e.g. F , t , r) with confidence intervals, effect sizes, degrees of freedom and P value noted
Give P values as exact values whenever suitable.
- For Bayesian analysis, information on the choice of priors and Markov chain Monte Carlo settings
- For hierarchical and complex designs, identification of the appropriate level for tests and full reporting of outcomes
- Estimates of effect sizes (e.g. Cohen's d , Pearson's r), indicating how they were calculated

Our web collection on [statistics for biologists](#) contains articles on many of the points above.

Software and code

Policy information about [availability of computer code](#)

Data collection

Next-generation sequencing of exome and targeted amplicon libraries was conducted on the Illumina platform (Illumina Inc, California, USA). Prioritization of mutation targets for design and application of personalized ctDNA assays was conducted by Natera Inc (San Carlos, USA).

Data analysis

Sequence data was aligned to human reference genome version GRCh38 using Burrows-Wheeler Alignment tool (version 0.7.12). Somatic mutations were detected for each tumor and PBL data pair using Varscan2, GATK MuTect2 and HaplotypeCaller (version 3.6-0-g89b7209), MuTect, and Vardict. Tumor mutation burden was calculated as the total number of nonsynonymous mutations detected in more than 2 out of 5 mutation callers for each sample. MSI status was determined for each tumor and normal using mSINGs with provided list of microsatellite genomic loci mapped to the GRCh38 reference using the UCSC LiftOver utility (<https://genome.ucsc.edu/cgi-bin/hgLiftOver>) and default parameters and detection cut-off. All statistical analyses were performed using R (R Foundation for Statistical Computing, Vienna, Austria; URL <https://www.R-project.org/>). Code necessary to reproduce the core analyses are available at <https://github.com/pughlab/inspire-ctdna>.

Multiplex PCR primer pairs targeting 16 highly ranked tumor-specific variants were designed as previously described. The primer sequences for each variant are from the Signatera assay and are proprietary of Natera. Somatic small nucleotide variants (SNVs) present in the tumor but absent in the germline were used to select the 16 targets, with prioritization based upon multiple factors, including the observed variant allele frequency in the tumor tissue and the associated background noise profile in the plasma. This prioritized list of variants was then used to design PCR amplicons based on optimized design parameters, ensuring uniqueness in the human genome, amplicon efficiency, and primer interaction. Next, multiplexed targeted PCR was conducted followed by amplicon deep sequencing on an Illumina platform. A sample was considered ctDNA positive when ≥ 2 out of the 16 selected target mutations were present at above a predefined threshold. Variant allele frequencies were determined for each of the 16 target mutations. Absolute ctDNA levels (mean tumor [ctDNA] molecules per mL [MTM/mL]) in the plasma were determined by normalizing variant allele frequencies by the plasma volume used for each sample. At each time point, MTM/mL was calculated from all 16 tested targets (including undetected targets).

For manuscripts utilizing custom algorithms or software that are central to the research but not yet described in published literature, software must be made available to editors/reviewers. We strongly encourage code deposition in a community repository (e.g. GitHub). See the Nature Research [guidelines for submitting code & software](#) for further information.

Data

Policy information about [availability of data](#)

All manuscripts must include a [data availability statement](#). This statement should provide the following information, where applicable:

- Accession codes, unique identifiers, or web links for publicly available datasets
- A list of figures that have associated raw data
- A description of any restrictions on data availability

Anonymized whole exome sequencing data of tumor and match normals are available with controlled access approval through the European Genome-Phenome Archive (EGA) under accession number EGAS00001003280. Source Data for Figures 1-6 can be found in Source Data Fig. 1-6 files, and Source Data for Extended Data Figures 2-8 can be found in Source Data Extended Data Fig. 2-8 files. The supporting variant level data for all figures are available in Supplementary Table 4. All other data supporting the findings of this study are available from the corresponding author on reasonable request.

Field-specific reporting

Please select the one below that is the best fit for your research. If you are not sure, read the appropriate sections before making your selection.

- Life sciences Behavioural & social sciences Ecological, evolutionary & environmental sciences

For a reference copy of the document with all sections, see nature.com/documents/nr-reporting-summary-flat.pdf

Life sciences study design

All studies must disclose on these points even when the disclosure is negative.

Sample size	Sample size calculation was not performed. Sample size was chosen based on budgetary considerations. For a given sample size, the minimum detectable effect size depends on the ctDNA positivity rate and the primary endpoint of PFS event rate within the cohort. We determined that our sample size was sufficient based on a power calculation with the following assumptions. Given a sample size of 106, ctDNA positivity rate of 80%, and PFS event rate of 75%, we would be powered to detect a clinically significant hazard ratio of 2.2 with 80% power at a two-sided significance level of 0.05.
Data exclusions	No data was excluded from the analysis.
Replication	Due to sample size and biospecimen availability, ctDNA measurements were performed once on each sample and were not repeated. Specific measures taken to verify the reproducibility of all the experiments included: 1) With each experiment, one in-line batch negative control sample going from library prep through sequencing; 2) Standard 45 SNP mPCR assays within each Signatera patient-specific mPCR reaction to confirm genotype concordance and contamination check for each plasma sample against genotypes generated in matched normal whole-exome sequencing data; 3) Signatera sequencing run-level controls to monitor run-to-run Signatera-specific QC metrics; 4) Illumina PhiX library sequencing run calibration control for run quality monitoring (cluster generation, sequencing, and alignment).
Randomization	There is no randomization as part of this study. Participants were enrolled into one of five sub-cohorts: (A) Squamous Cell Cancer of Head and Neck (SCCHN); (B) Triple Negative Breast Cancer (TNBC); (C) Epithelial Ovarian Cancer (EOC) Type II; (D) Malignant Melanoma (MM); or (E) Mixed Advanced Solid Tumors. This was conducted because the event rate for PFS, OS, and objective response were assumed to be distinct for each of these sub-cohorts. The sub-cohorts was used as a covariate in multivariable models to account for this.
Blinding	The ctDNA measurements were conducted by Natera in a manner that kept them blinded to clinical data including PFS, OS, and objective response. All treatment and clinical management decisions were made blinded to ctDNA results. All clinical outcome data were collected by individuals blinded to the ctDNA results.

Reporting for specific materials, systems and methods

We require information from authors about some types of materials, experimental systems and methods used in many studies. Here, indicate whether each material, system or method listed is relevant to your study. If you are not sure if a list item applies to your research, read the appropriate section before selecting a response.

Materials & experimental systems

n/a	Involved in the study
<input type="checkbox"/>	<input checked="" type="checkbox"/> Antibodies
<input checked="" type="checkbox"/>	<input type="checkbox"/> Eukaryotic cell lines
<input checked="" type="checkbox"/>	<input type="checkbox"/> Palaeontology
<input checked="" type="checkbox"/>	<input type="checkbox"/> Animals and other organisms
<input type="checkbox"/>	<input checked="" type="checkbox"/> Human research participants
<input type="checkbox"/>	<input checked="" type="checkbox"/> Clinical data

Methods

n/a	Involved in the study
<input checked="" type="checkbox"/>	<input type="checkbox"/> ChIP-seq
<input checked="" type="checkbox"/>	<input type="checkbox"/> Flow cytometry
<input checked="" type="checkbox"/>	<input type="checkbox"/> MRI-based neuroimaging

Antibodies

Antibodies used	For PD-L1 immunohistochemistry, staining and central assessment was conducted by QualTek Molecular Laboratories (Newtown, PA, USA) using PD-L1 monoclonal antibody clone 22C3 at a concentration of 2 μ g/mL.
Validation	QualTek Molecular Laboratories has previously validated an immunohistochemistry assay for PD-L1 using the Merck & Co., Inc (Merck) proprietary mouse monoclonal antibody clone 22C3 for the testing of formalin-fixed, paraffin-embedded (FFPE) tissues (Dolled-Filhart M. et. Al., Archives of Pathology & Laboratory Medicine: Nov. 2016, Vol. 140, No. 11, pp. 1259-1266; http://dx.doi.org/10.5858/arpa.2015-0544-OA).

Human research participants

Policy information about [studies involving human research participants](#)

Population characteristics	Patients \geq 18 years of age with advanced solid tumors and available archived or baseline tumor tissue provided informed consent were enrolled in this single-arm phase 2 study. Participants were enrolled into one of five sub-cohorts: (A) Squamous Cell Cancer of Head and Neck (SCCHN); (B) Triple Negative Breast Cancer (TNBC); (C) Epithelial Ovarian Cancer (EOC) Type II; (D) Malignant Melanoma (MM); or (E) Mixed Advanced Solid Tumors. Participants were required to have measurable disease, ECOG status 0-1, and adequate organ function. Participants could not have had prior anti-PD1/PDL1/PDL2 therapy or active immunodeficiency, auto-immune disease, pneumonitis, active tuberculosis, or active central nervous system metastases. Details regarding patient age (median 59 years), sex (62% female), ethnicity, sub-cohort, and prior lines of treatment are provided in Supplementary Tables 2 and 3.
Recruitment	Patients were recruited at clinics in Princess Margaret Cancer Centre (University Health Network), a research hospital in downtown Toronto, Ontario. As patients were expected to allow on-treatment biopsies and provide research blood samples, the recruited population likely represented on average a healthier and better prognosis group than an average clinical presentation off study. This self-selection bias could result in altered effect sizes of prognostic and predictive biomarkers such as ctDNA.
Ethics oversight	Research Ethics Board at University Health Network

Note that full information on the approval of the study protocol must also be provided in the manuscript.

Clinical data

Policy information about [clinical studies](#)

All manuscripts should comply with the ICMJE [guidelines for publication of clinical research](#) and a completed [CONSORT checklist](#) must be included with all submissions.

Clinical trial registration	NCT02644369
Study protocol	The full protocol is available from the authors upon reasonable request.
Data collection	Patients accrual and data collection was conducted at Princess Margaret Cancer Centre (University Health Network). Accrual was from March 21, 2016 to May 9, 2018. The data collection cut-off date was July 18, 2019.
Outcomes	<p>A statistical analysis plan was designed prior to data analysis. The primary outcome was progression free survival (PFS), and overall survival (OS) was the secondary endpoint. In the primary analysis, data from all 5 sub-cohorts were combined and analyzed as a single cohort for evaluation. We hypothesized that the presence of ctDNA at the baseline and post-treatment would be associated with decreased PFS and OS.</p> <p>Other endpoints of the INSPIRE protocol include the change in genomics and immune landscapes, RNA expression correlates of treatment response, radiomic imaging analysis, and tumor penetration of pembrolizumab as determined by mass spectrometry. Adverse events were monitored throughout the trial and graded in severity according to guidelines outlined in the NCI Common Terminology Criteria for Adverse Events (CTCAE) version 4.03. After the end of treatment, each subject was followed for 30 days for adverse event monitoring (serious adverse events was collected for 90 days after the end of treatment).</p>